

# AE-GAN: adversarial eliminating with GAN

Shiwei Shen  
ICT\*

shenshiwei@ict.ac.cn

Guoqing Jin  
ICT\*

jinguoqing@ict.ac.cn

Ke Gao  
ICT\*

kegao@ict.ac.cn

Yongdong Zhang  
ICT\*

zhyd@ict.ac.cn

## Abstract

Although Neural networks could achieve state-of-the-art performance while recognizing images, they often suffer a tremendous defeat from adversarial examples—inputs generated by utilizing imperceptible but intentional perturbations to samples from the datasets. How to defend against adversarial examples is an important problem which is well worth to research. So far, only two well-known methods adversarial training and defensive distillation have provided a significant defense. In contrast to existing methods mainly based on model itself, we address the problem purely based on the adversarial examples itself. In this paper, a novel idea and the first framework based Generative Adversarial Nets named AE-GAN capable of resisting adversarial examples are proposed. Extensive experiments on benchmark datasets indicate that AE-GAN is able to defend against adversarial examples effectively.

## 1 Introduction

Deep neural networks have recently achieved excellent performance on a variety of visual and speech recognition tasks[4, 8, 14] mainly because they can approximate any function to an arbitrary degree of accuracy with enough hidden layers[10]. However, they have non-intuitive characteristics and intrinsic blind spots that are easy to attack using obscure manipulation of their input[1, 6, 15, 20, 24]. In many cases, the structure of the neural model is strongly related to the training data distribution, which is in contradiction with the network's

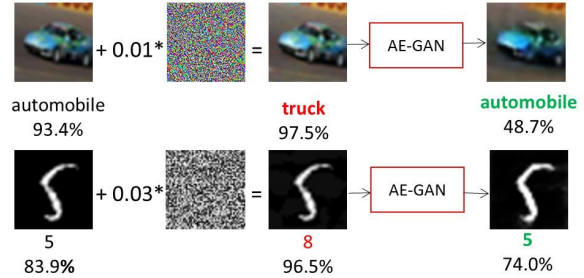


Figure 1: A demonstration of AE-GAN applied to MNIST and CIFAR10 classify network. The image can be incorrectly classified with a small perturbation. The adversarial image processed by our model is able to be classified correctly by the original network.

ability to achieve high generalization performance.

Szegedy etc. find that imperceptible perturbation of test samples can be misclassified by neural networks[24]. They term this kind of subtle perturbed sample “*adversarial examples*”. In contrast to noise samples, adversarial examples are imperceptible, designed intentionally, and more likely to cause false predictions. What is more serious is that an adversarial example customized for one machine learning model is often misclassified by various models with distinct architectures trained on different subsets of the samples.

Adversarial examples pose potential security threats for practical machine learning applications. An attack utilizing adversarial examples can be performed even if the attacker has no access to the underlying model[7]. Nguyen etc.[18] design a category of evolved images that are unrecognizable to humans cause DNN discriminative model to make a mistake. Recent research has shown that adver-

\*Institute of Computing Technology Chinese Academy of Sciences, Beijing 100190, China

arial examples can be constructed in the physical world and photographed through a smartphone[15]. This makes it possible to allow an adversary to produce images of traffic signs misclassified by the autonomous vehicles driving system[21]. Therefore, the study of preventing adversarial examples is significant and very urgent.

The view that neural networks linear behavior in high-dimensional primary cause the adversarial perturbation[6] has been widely accepted. When the infinitesimal perturbations being highly aligned with the weight vectors, the model most likely accumulates one large change to the output.

Traditional strategies such as pretraining and dropout are not conducive to improving the models robustness to adversarial examples. Adversarial training, that back-feeds adversarial examples to training, does provide an additional regularization benefit of the resulting models, but fails to reduce the model's vulnerability to adversarial perturbations. The failure of this methods mainly because they make efforts to regularize the network to better fit the ditribution of adversarial examples, which bring no change to the function of the classifier itself, thus does not eliminate the high-dimensional linear properties of the model that the primary cause of neural networks' vulnerability to adversarial perturbation.

Since the high-dimensional linear nature of the model can hardly be avoided in practical application, it becomes more difficult to defend against adversarial examples. But the generalization of adversarial examples across different models provides new ideas and methods to solve the problem of adversarial attack. Compared with clean examples, adversarial examples contain infinitesimal perturbations that add up to one large change to the output[6]. It is possible to prevent adversarial examples if there is an algorithm that can dispel or damage the infinitesimal perturbations of the samples.

Generative Adversarial Nets(GANs) allows one to generate an image with similar distribution to the training set with a random input vector. The idea of using GANs to learn a mapping from adversarial examples' manifold to clean examples' originates from [17].

In this paper, a novel framework based Generative Adversarial Nets is proposed to weaken the aggressivity of adversarial examples before being recognized by the machine learning systems. The training procedure of generative component is to dispel or damage the input sam-

ples' adversarial perturbations being highly aligned with the weight vectors of the models. To achieve this, a task specified loss function is invented to make the adversarial examples being high consistent with the clear samples.

The contributions of this paper can be summarized as follows:

**(1) A novel idea of defending against adversarial examples is proposed.** The aggressivity of adversarial examples can be undermined via the elimination of the trivial perturbations of the input data being highly aligned with the weight vectors of the models.

**(2) It is the first framework based Generative Adversarial Nets capable of preventing adversarial examples.** A task specified loss function is invented to achieve this objective.

**(3) The proposed framework possesses strong applicability.** It is able to allow various networks with different hyper-parameters trained on a disjoint training set to resist adversarial attacks.

**(4) The training procedure of the proposed framework needs no knowledge of the architecture and parameter values of the potentially attacked models.**

## 2 Related Work

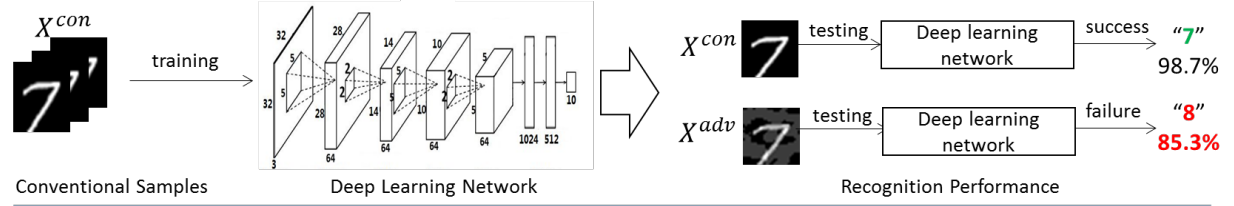
In this section, methods of generation and defense against adversarial examples that are closely related to this work is briefly reviewed. In addition, Generative Adversarial Nets(GANs) and its connection to our method will be discussed.

### 2.1 Methods Generating Adversarial Examples

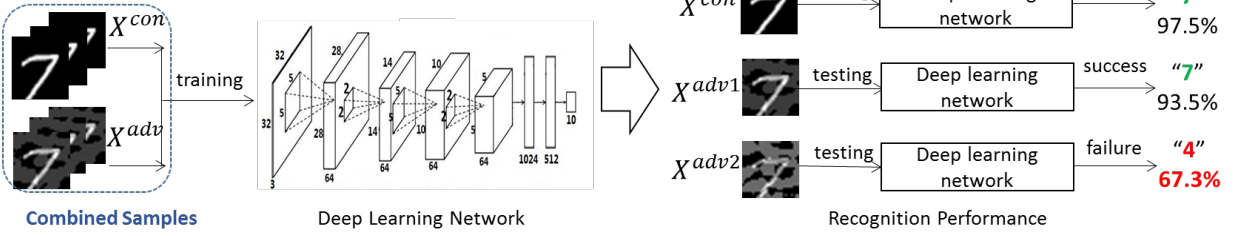
In the remaining of the paper we use the following notation and terminology:

- $X$  - the clean image from the dataset.
- $X^{adv}$  - the adversarial image, the intentional perturbations of the clean image.
- $y_{true}$  - true class for the input  $X$ .
- $f$  - classifier mapping from input image to a discrete label set.

(a) Traditional Deep Learning Framework



(b) Existing Adversarial Training Framework



(c) Our Adversarial Eliminating Framework

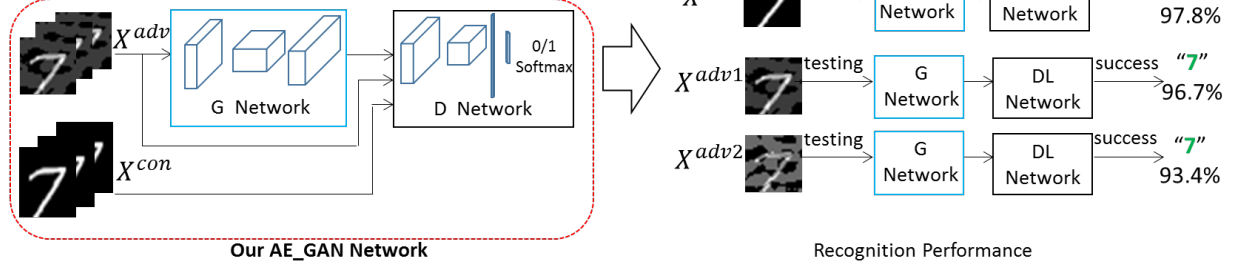


Figure 2: The proposed adversarial perturbation elimination networks(AE-GAN). The traditional deep learning framework possesses no ability of resisting adversarial examples. Existing adversarial training frameworks can somewhat increase the robustness of the models. We propose a adversarial eliminating framework AE-GAN to undermine the infinitesimal perturbation of the adversarial examples before it be feed into the deep learning models.

- $J(X, y_{true})$  - the cost function used to train the model given image  $X$  and class  $y$ .
- $\epsilon$  - the size of worst-case perturbations,  $\epsilon$  is the upper bound of the  $L_\infty$  norm of the perturbations.
- $Clip_{X,\epsilon}\{A\}$  - an  $\epsilon$ -neighbourhood clipping of  $A$  to the range  $[X_{i,j} - \epsilon, X_{i,j} + \epsilon]$ .

Construction of an adversarial example can be formulated as a small enough perturbation  $\epsilon$  of input  $x$  and  $x_\epsilon$  that satisfies  $\|x - x_\epsilon\| < \epsilon$  but  $f(x) \neq f(x_\epsilon)$ .

Methods generating adversarial examples can be categorized as single-step method and iterative method. Iterative method is a straightforward extension of single-step method is to apply it multiple times, which seems to be more rejective.

**Single-step Method:** Minimum distortion generation function  $D$  where  $f(D(x)) \neq f(x)$  defined as an optimization problem is solved by a box-constrained L-BFGS to craft adversarial perturbation[24]. Inspired by the linear explanation, Goodfellow et al.[6] propose the *fast gradient sign method*(FGSM), which linearizes the cost function and solve the optimal max-norm constrained perturbation:

$$X^{adv} = X + \epsilon \text{sign}(\nabla_X J(X, y_{true})) \quad (1)$$

This method is more simple and efficient than L-BFGS, but lower attack success rate.

**Iterative Method:** An straightforward way to extend the FGSM is to multiple times with small step size:

$$\begin{aligned} X_0^{adv} &= X, \\ X_{N+1}^{adv} &= Clip_{X,\epsilon}\{X_N^{adv} + \\ &\quad \alpha \text{sign}(\nabla_X J(X_N^{adv}, y_{true}))\} \end{aligned} \quad (2)$$

where  $\alpha$  is the amount of pixel value change on each step. It requires an heuristic iterative procedure to computer the adversarial exmaples[15]. It is employed to generate the iterative adversarial examples  $X_i^{adv}$  in our exmpperiments. An alternative approach is to specify which of the incorrect classes the model should select. The *iterative least-likely class method*[15] is introduced to make an avdversarial example which will be classified as desired class:

$$\begin{aligned} X_0^{adv} &= X, \\ X_{N+1}^{adv} &= Clip_{X,\epsilon}\{X_N^{adv} - \\ &\quad \alpha \text{sign}(\nabla_X J(X_N^{adv}, y_{LL}))\} \end{aligned} \quad (3)$$

where  $y_{LL}$  is the least-likely class according to the prediction of the model.

A subtle, but essential notation is that there is no guarantees that adversarial examples generated by above methods will be actually misclassified.

## 2.2 Adversarial Examples Defense

Traditional techniques that improve the stability of neural networks, such as data augmentation, dropout, weight decay and regularization, generally are statistically inefficient against adversarial examples[6, 24]. So far, only two well-known methods have provided a significant defense.

### 2.2.1 Adversarial training

Adversarial training is a brute force solution where a great many of adversarial examples are feedbacted to train the models. A neural network could be regularized somewhat by adversarial training. But the lack of adversarial examples limits the regularization. An effective regularizer training with an adversarial objective function based on FGSM is proposed in [6]:

$$\begin{aligned} \tilde{J}(\theta, x, y) &= \alpha J(\theta, x, y) + \\ &\quad (1 - \alpha) J(\theta, x + \epsilon \text{sign}(\nabla_x J(\theta, x, y)), y) \end{aligned} \quad (4)$$

which implies that adversarial examples are continually updated during the training procedure. It could achieve better performance than training on a static mixture of adversarial and clean examples. This strategy is employed in our experiment to supply enough adversarial examples.

An open-source implementation of adversarial training is available in the *cleverhans* library[19]. But adversarial training does not grant a satisfactory reduction in vulnerability to adversarial examples. If we instead use adversarial examples designed to perturb the adversarially trained models, the error rate of misclassification is no significant decline.

### 2.2.2 Defensive distillation

Defensive distillation[22] is another well-known model for resisting adversarial examples which is an alternative defense strategy where we train the model to output probabilities of different classes, rather than hard decisions

about which class to output. The probabilities are supplied by an earlier model, trained on the same task using hard class labels. This creates a model whose surface is smoothed in the directions an adversary will typically try to exploit, making it difficult for them to discover adversarial input tweaks that lead to incorrect categorization. Distillation was originally introduced in [9] as a technique for model compression, where a small model is trained to imitate a large one, in order to obtain computational savings.

Defensive distillation is trained in three steps:

1. Train a network (the *teacher*) using standard techniques. In this network, the output is given by  $F(\theta, x) = \text{softmax}(Z(\theta, x)/T)$  Here,  $T$  is the temperature. As  $T \rightarrow \infty$  the distribution approaches uniform;  $T = 1$  is used by standard softmax.
2. Evaluate the *teacher* network on each instance of the training set to produce *soft labels*.
3. Train a second network (the *distilled* network) on the *soft labels* again using temperature  $T$ . By training on the *soft labels*, the model should overfit the data less and try to be more regular.

## 2.3 Generative Adversarial Nets

Generative Adversarial Nets (GAN)[5] is a framework incorporating an adversarial discriminator into the procedure of training generative models. The method implements two networks against each another: a generator  $G$  that is optimized to estimate the data distribution and a discriminator  $D$  that aiming to distinguish between samples from the training data and fake samples from  $G$ .

The training procedure for  $G$  is to produce an example from random noise potentially to deceive  $D$ , for  $G$  is to maximize the probability of tell apart real data examples from generative examples. The generator  $G$  is rewarded for producing examples that did fool the discriminator and the discriminator for correct classifications. The generator and discriminator play a zero sum game. The objective can be stated using a minimax value function[5]:

$$\min_G \max_D (E_{X \sim p_{\text{data}}(X)} [\log D(X)] + E_{z \sim p_z(z)} [\log(1 - D(G(z)))] ) \quad (5)$$

Both generator  $G$  and discriminator  $D$  are trained by backpropagating the loss in Eqn. 5 to update the parameters.

The Deep Convolutional Generative Adversarial Nets (DCGAN)[23] is an straightforward extension of the GAN with convolutional networks that makes them stable to train in most settings. Our model in the paper is implemented based on DCGAN for resisting adversarial perturbations, and the details will be discussed in the following Section.

## 3 Method

The fundamental ideas of defending against adversarial examples is to eliminate or damage of the trivial perturbations of the input data being highly aligned with the weight vectors of the models. The infinitesimal difference of adversarial image and clean image can be formulated as:

$$\|X^{adv} - X\| = \eta \quad (6)$$

Ideally, the perturbations  $\eta$  can be get rid from  $X^{adv}$ . That means the distribution of  $X^{adv}$  is highly consistent with  $X$ .

The global optimality of GANs is the generative distribution of  $G$  consistent with samples from the data generating distribution:

$$p_g = p_{\text{data}} \quad (7)$$

The procedure of converging to a good estimator of  $p_{\text{data}}$  coincides with the demand of the elimination of adversarial perturbations  $\eta$ .

Based on the above analysis, a novel framework based GANs to undermine the infinitesimal perturbations of the input data that add up to one large change to the output is proposed. We name this class of architectures defending against adversarial examples based on GANs (AE-GAN).

The AE-GAN network is trained in an adversarial setting. While the generator  $G$  is trained to alter the perturbation with tiny changes to the input examples, the discriminator  $D$  is optimized to separate the adversarial examples and clean examples. To achieve this, a task specified fusion loss function is invented to make the adversarial examples being high consistent with original input image manifold.

### 3.1 Architecture

The ultimate goal of AE-GAN is to train a generating function  $G$  that estimates for a given adversarial input image  $X^{adv}$  its corresponding  $\hat{X}$  counterpart. To achieve this, a generator network parametrized by  $\theta_G$  is trained, here  $\theta_G$  denotes the weights and biases of a generate network and is obtained by optimizing a adversarial elimination specified loss function  $l_{ae}$ . For training images  $X_n^{adv}$  obtained by applying FGSM with corresponding original iclean mage  $X_n$ ,  $n = 1, \dots, N$ , we solve:

$$\hat{\theta}_G = \arg \min_{\theta_G} \frac{1}{N} \sum_{n=1}^N l_{slack}(G_{\theta_G}(X_n^{adv}), X_n) \quad (8)$$

A discriminator network  $D_{\theta_D}$  along with  $G_{\theta_G}$  is defined to solve the adversarial zero sum problem:

$$\min_{\theta_G} \max_{\theta_D} \mathbb{E}_{X \sim p(X)} \log D_{\theta_D}(X) - \mathbb{E}_{X^{adv} \sim p_G(X^{adv})} \log(D_{\theta_D}(G_{\theta_G}(X^{adv}))) \quad (9)$$

The general idea behind this formulation is that it allows one to train a generative model  $G$  with the goal of deceiting a differentiable discriminator  $D$  that is train to tell apart adversarial images from original clean images. Thus the generator can be trained to produce adversarial perturbation blocking images that are highly similar to original clean images, and thus it difficult to distinguish by  $D$ .

The architecture of our generator network  $G$  is illustrated in Figure 2. We use two convolutional layers with  $3 \times 3$  kernels and 64 feature maps followed by two deconvolutional layers and ReLU as the activation function.

To discriminate original clean images from generated adversarial perturbation blocking samples, we train a discriminator network. The general architecture is illustrated in Figure 2. The discriminator network is trained to solve the maximization problem in Equation 9. It contains  $X$  convolutional layers. The resulting  $X$  feature maps are followed by two dense layers and a final sigmoid activation function to obtain a probability for sample classification.

### 3.2 Loss Function

The definition of our adversarial elimination specified loss function  $l_{ae}$  is critical for the performance of our genera-

tor network to produce images without adversarial perturbations. We define  $l_{ad}$  as the weighted sum of several loss functions as:

$$l_{ae} = \xi_1 l_{mse} + \xi_2 l_{adv} + \xi_3 l_{sc} \quad (10)$$

where consist of pixel-wise MSE(mean square error) loss, adversarial loss and spatially coherent loss.

Inspired by image super resolution method[3] the pixel-wise MSE loss is defined as:

$$l_{mse} = \frac{1}{WH} \sum_{x=1}^W \sum_{y=1}^H (X_{x,y} - G_{\theta_G}(X^{adv})_{x,y}) \quad (11)$$

Adversarial perturbations can be viewed as a special noise constructed delicately. The most widely used loss for image denoise or super resolution will be able to achieve satisfactory results for adversarial elimination.

To encourage our network to produce images residing on the manifold of original clean images, the generative loss of the GAN is also employed. The generative loss  $l_{adv}$  is calculated based on the probabilities of the discriminator over all adversarial images as:

$$l_{adv} = \sum_{n=1}^N [1 - \log D_{\theta_D}(G_{\theta_G}(X^{adv}))] \quad (12)$$

In addition to the adversarial loss, we also add a spatially coherent loss based on the total variation to  $l_{ae}$ , which is calculated as:

$$l_{sc} = \frac{1}{WH} \sum_{x=1}^W \sum_{y=1}^H \|\nabla G_{\theta_G}(X^{adv})_{x,y}\| \quad (13)$$

This formulation encourages one to generate an adversarial slack image with infinitesimal and imperceptible changes to a adversarial sample.

## 4 Experiments

We perform experiments on MNIST[16] and CIFAR-10[13] and the German Traffic Sign Recognition Benchmark (GTSRB) datasets. The MNIST datasets has 60,000 training examples and 10,000 test examples. The CIFAR-10 consists of about 50,000 color training images and



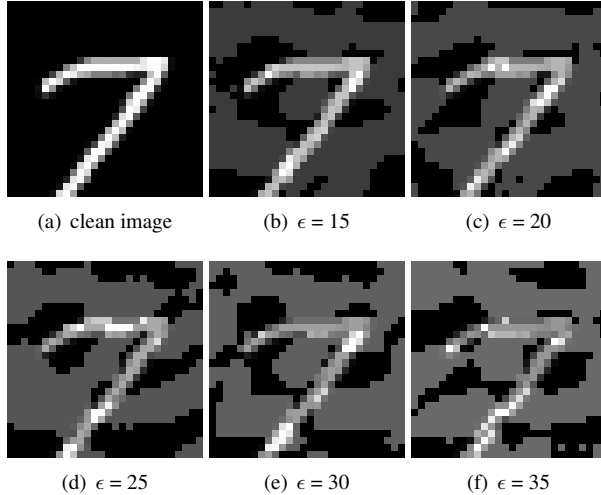


Figure 3: Comparison of adversarial images from MNIST with different noise scale  $\epsilon$ .

10,000 test images. The GTSRB is an image collection consisting of 43 traffic signs [11]. Images vary in size and are RGB-encoded. To simplify, we resize images to 32x32 pixels. We keep 30,000 images for our training set and 9,209 for our test set (out of the 39,209 available). FGSM[19] is employed to generate various adversarial images with different noise scale controlled by parameter  $\epsilon$ . The higher values of  $\epsilon$  exploit much finer perturbations which confuse the classifier with higher rate. The adversarial samples from MNIST and CIFAR-10 with various noise scale  $\epsilon$  are shown in Figure 3 and Figure 4. Adversarial images with large noise scale essentially are essentially destroyed and become unrecognisable even by humans.

#### 4.1 Substitute Model Training

It is more easy to exploit much finer perturbations to confuse the classifier with higher rate when attacker has full access to the model (i.e. the architectures, model weights). However, most of the realistic security threats are black box scenario, in which adversary has no knowledge of the models. As adversarial examples transfer between architectures, black-box attacks can be accom-

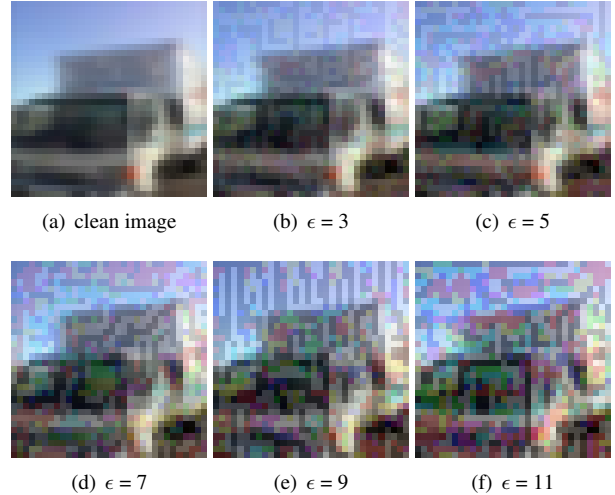


Figure 4: Comparison of adversarial images from MNIST with different noise scale  $\epsilon$ .

plished at a much lower cost[21].

To perform a real-world and properly-blinded evaluation, a substitute model approximating the target of being attacked is constructed. Adversarial examples are then crafted using the substitute rather than the target model.

Three classify models  $\text{ConvNet}_i$  ( $i = 1, 2, 3$ ) with different architectures and weights are constructed as the substitute candidates.  $\text{ConvNet}$  (the original Keras CIFAR-10  $\text{ConvNet}$ [2]) is the network of attack. Table 1 shows the details and other variants of network architectures. The accuracy of the three substitute models is reported in Table 2. It is computed with the CIFAR-10 test data set. The classify accuracy of  $\text{ConvNet}_i$  is much lower than the original  $\text{ConvNet}$ .

However, the difference of the architectures and the performance does not bring any difficulty for the adversary to learn a substitute capable of mimicking the decision boundaries of  $\text{ConvNet}$ . The proportion of adversarial samples crafted by the substitute  $\text{ConvNet}_i$  are misclassified by the  $\text{ConvNet}$  is 62.4%, 58.9% and 60.0% respectively. Therefore, an effective attack can be conducted even if the adversary have no full knowledge of potentially attacked network.

Table 1: CIFAR-10 ConvNet configurations (shown in columns). The ReLU activation function is not shown for brevity. The convolutional layer parameters are denoted as “conv<receptive field size>- <number of channels>”.

CIFAR-10 ConvNet Classifier Model			
ConvNet	ConvNet1	ConvNet2	ConvNet3
conv3-32	conv3-32	conv3-32	conv3-32
conv3-32	conv3-32		conv3-32
maxpool			
conv3-64	conv3-64	conv3-64	conv3-64
conv3-64	conv3-64		conv3-64
maxpool			
FC-512	conv3-128	conv3-128	conv3-128
	conv3-128	maxpool	maxpool
	maxpool	FC-1024	FC-512
	FC-1024		FC-4096
FC-10			
softmax			

Table 2: Top-1 classification accuracy on the CIFAR-10 clean test images. The classification accuracy of substitute models ConvNet $i$  ( $i = 1, 2, 3$ ) is lower than the target model ConvNet.

ConvNet	ConvNet1	ConvNet2	ConvNet3
0.720	0.674	0.647	0.658

Table 3: Training configurations of the AE-GAN. MNIST, CIFAR-10, GTSRB are trained separately.

	MNIST	CIFAR-10	GTSRB
Learning Rate	0.0002	0.0002	0.0002
Momentum	0.5	0.5	0.5
Epoch	2	10	10
Input Size	64*28*28*1	64*32*32*3	64*32*32*3

## 4.2 Comparison

The ConvNet1 model is employed substituting for the target ConvNet[2] to crafted adversarial examples of CIFAR-10. While we employed ConvNet to generate adversarial images to confuse cleverhans MNIST classifier[19].

### 4.2.1 Training and Parameters

The straightforward method to train the generator and the discriminator is update both in every batch. However, the discriminator network often learns much faster than the generator network because the generator is more complex than distinguish between real and fake. Therefore, generator should be run twice with each iteration to make sure that the loss of discriminator does not go to zero. This method significantly help to produce better results. Adam[12] is used to update parameters and optimize the networks with batch size of 64. The weights of the adversarial elimination specified loss  $\xi_1$ ,  $\xi_2$  and  $\xi_3$  used in the Eqn. 10 are fixed to 0.1, 0.45, 0.45 separately. Other parameters related to training are shown in Table. 3.

The iterative adversarial examples  $X_i^{adv}$  is crafted using Eqn. 2. It is important to note that the samples become more and more aggressive as the number of iterations increases. To increase the robustness of the models against adversarial examples generated by iterative methods, adversarial training  $Model_i^{adv}$  had to feedback all the iterative adversarial examples  $X_0^{adv}, X_1^{adv}, \dots, X_i^{adv}$  to make them resist the current version of the model.  $Model_0^{adv}$  represents original models with our adversarial training. In the following experiment, we use  $\epsilon = 15$  for MNIST,  $\epsilon = 5$  for CIFAR-10 and GTSRB.



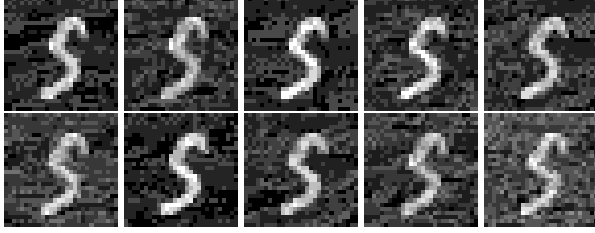


Figure 5: The adversarial examples regarded as weapons of attacker with different attack intensity

Table 4: The training time(s), epoch and samples number of methods in MNIST datasets

	training time(s)	epoch	samples number
$Model_0^{adv}$	38.05	5	60,000
$Model_1^{adv}$	82.81	5	120,000
$Model_2^{adv}$	126.38	5	180,000
$Model_3^{adv}$	176.86	5	240,000
$Model_4^{adv}$	221.77	5	300,000
Ours	119.38	5	60,000

Table 5: The training time, epoch and samples number of methods in CIFAR-10 datasets

	training time(s)	epoch	samples number
$Model_0^{adv}$	246.96	20	50,000
$Model_1^{adv}$	707.14	20	100,000
$Model_2^{adv}$	869.86	20	150,000
$Model_3^{adv}$	1596.54	30	200,000
$Model_4^{adv}$	2674.84	40	250,000
Ours	950.75	10	50,000

Table 6: Top-1 accuracy of different attack intensity in the MNIST datasets. **Ours** means the adversarial examples should be reconstructed with our AE-GAN before classified by the  $Model_0^{adv}$ .

	$X_1^{adv}$	$X_2^{adv}$	$X_3^{adv}$	$X_4^{adv}$	$X_5^{adv}$
$Model_0^{adv}$	0.752	0.293	0.249	0.246	0.241
$Model_1^{adv}$	0.923	0.670	0.560	0.520	0.485
$Model_2^{adv}$	0.948	0.915	0.772	0.724	0.652
$Model_3^{adv}$	0.941	0.927	0.855	0.810	0.761
$Model_4^{adv}$	0.946	0.929	0.862	0.829	0.798
Ours	<b>0.974</b>	<b>0.966</b>	<b>0.933</b>	<b>0.891</b>	<b>0.840</b>

Table 7: Top-1 accuracy of different attack intensity in the CIFAR-10 datasets. **Ours** means the adversarial examples should be reconstructed with our AE-GAN before classified by the  $Model_0^{adv}$ .

	$X_1^{adv}$	$X_2^{adv}$	$X_3^{adv}$	$X_4^{adv}$	$X_5^{adv}$
$Model_0^{adv}$	0.375	0.314	0.270	0.249	0.246
$Model_1^{adv}$	0.582	0.575	0.566	0.550	0.540
$Model_2^{adv}$	0.584	0.581	0.574	0.559	0.548
$Model_3^{adv}$	0.596	0.588	0.580	0.569	0.560
$Model_4^{adv}$	0.606	0.602	0.593	0.583	0.574
Ours	<b>0.610</b>	<b>0.608</b>	<b>0.603</b>	<b>0.591</b>	<b>0.580</b>

#### 4.2.2 Result

Compared the  $X_i^{adv}$  according to the Figure 6, the accuracy is growing with including more adversarial examples to train. However, the training time of adversarial training is growing fast with the more adversarial examples included to train and the more iterations needed to better fitting the expanded training datasets according to Table 5 and Table 4.

The change curves of accuracy accompanied with attack intensity in both datasets are showed in the Figure 6 and the Figure 6. Our AE-GAN has a good performance of resisting the different level adversarial examples than others according to the above tables and figures.

The images size and images channels of GTSRB datasets are same with the CIFAR-10 datasets. So the adversarial samples of GTSRB datasets can be reconstructed by the AE-GAN trained with the CIFAR-10 datasets without trained on the GTSRB datasets which is named *Ours*<sup>-</sup>. For fair comparison, the AE-GAN is also trained on the GTSRB datasets which is named *Ours*.

The result of the GTSRB datasets is showed in the Table 8 and the Figure 7.

Compared with the  $Model_0^{adv}$  and *Ours*<sup>-</sup>, the result indicate that the AE-GAN can also gain better performance even if no knowledge of the architecture and the training datasets of the targeted models. In other words, the AE-GAN is able to allow various networks with different hyper-parameters trained on a disjoint training set to resist adversarial attacks.

The Table 9, 10 and 11 indicate that the AE-GAN gains better performance than Defensive Distillation.

The final result on the three benchmark datasets is shown in Table 12, 13, 14 and Figure 8, 9, 10 which demonstrate that AE-GAN the first framework based Generative Adversarial Nets can provide a significant defense on adversarial examples.

The Figure 14, 15, 13 indicate that the aggressivity of adversarial examples can be undermined via the elimination of the trivial perturbations of the input data.

In addition, the adversarial examples can also be reconstructed by the AE-GAN even if the knowledge of the architecture and parameter values of the potentially attacked models can't accessed.

Table 8: Accuracy of different attack intensity compared with Adversarial Training on the GTSRB datasets.  $Model_0^{adv}$  represents that the model is trained with clean image and no distillation. *Ours*<sup>-</sup> represents the model is just trained on the CIFAR-10 datasets without trained on the GTSRB datasets in order to convince that the AE-GAN can also gain better performance even if no knowledge of the architecture and the training datasets of the targeted models. **Adversarial training**  $Model_i^{adv}$  represents it had to include all the iterative adversarial examples  $X_0^{adv}, X_1^{adv}, \dots, X_i^{adv}$  to train. *Ours* represents the model is trained on GTSRB datasets.

	$X_1^{adv}$	$X_2^{adv}$	$X_3^{adv}$	$X_4^{adv}$	$X_5^{adv}$
$Model_0^{adv}$	0.545	0.509	0.471	0.449	0.424
<i>Ours</i> <sup>-</sup>	0.574	0.523	0.492	0.477	0.454
$Model_1^{adv}$	0.610	0.576	0.552	0.534	0.525
$Model_2^{adv}$	0.628	0.600	0.581	0.571	0.558
$Model_3^{adv}$	0.640	0.613	0.596	0.589	0.571
$Model_4^{adv}$	0.635	0.608	0.600	0.594	0.586
Ours	<b>0.667</b>	<b>0.631</b>	<b>0.608</b>	<b>0.598</b>	<b>0.587</b>

Table 9: Accuracy of different attack intensity compared with Defensive Distillation on the MNIST datasets.  $Model_0^{adv}$  represents that the model is trained with clean image and no distillation.  $T$  is the temperature of Defensive Distillation [22]. The best two results are shown in **red** and **blue**, respectively.

	$X_1^{adv}$	$X_2^{adv}$	$X_3^{adv}$	$X_4^{adv}$	$X_5^{adv}$
$Model_0^{adv}$	0.752	0.293	0.249	0.246	0.241
$T = 5$	0.833	0.392	0.312	0.306	0.290
$T = 15$	0.832	0.399	0.312	0.317	0.299
$T = 25$	0.845	0.458	0.376	0.365	0.356
$T = 45$	0.845	0.533	0.463	0.450	0.420
$T = 65$	<b>0.875</b>	<b>0.631</b>	<b>0.535</b>	<b>0.507</b>	<b>0.477</b>
$T = 85$	0.859	0.556	0.453	0.436	0.404
$T = 95$	0.841	0.537	0.445	0.425	0.403
Ours	<b>0.974</b>	<b>0.966</b>	<b>0.933</b>	<b>0.891</b>	<b>0.840</b>

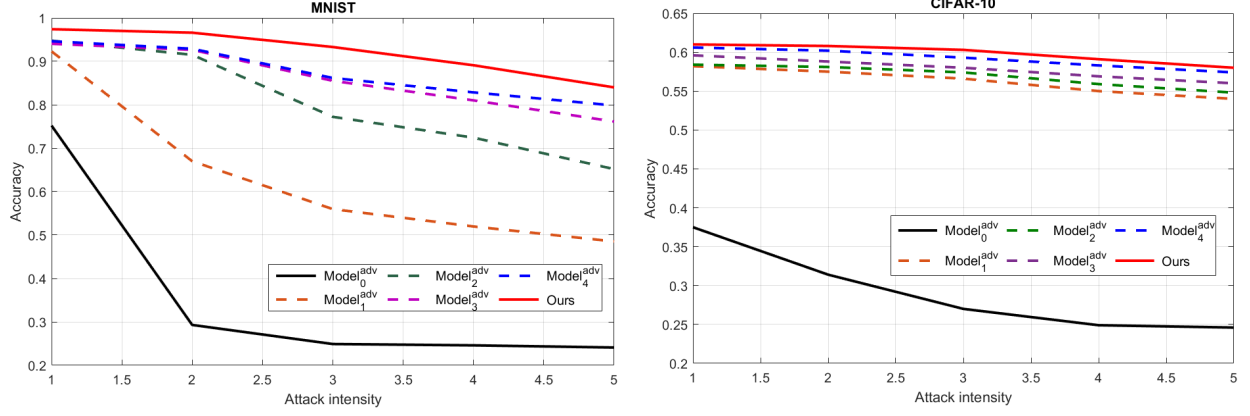


Figure 6: The change curves of accuracy accompanied with attack intensity in the MNIST datasets and CIFAR-10 datasets

Table 10: Accuracy of different attack intensity compared with Defensive Distillation on the CIFAR-10 datasets.  $Model_0^{adv}$  represents that the model is trained with clean image and no distillation.  $T$  is the temperature of Defensive Distillation [22]. The best two results are shown in red and blue, respectively.

	$X_1^{adv}$	$X_2^{adv}$	$X_3^{adv}$	$X_4^{adv}$	$X_5^{adv}$
$Model_0^{adv}$	0.375	0.314	0.270	0.249	0.246
$T = 5$	0.335	0.289	0.236	0.223	0.219
$T = 15$	0.351	0.313	0.277	0.258	0.242
$T = 25$	0.353	0.321	0.277	0.262	0.253
$T = 45$	0.419	0.400	0.375	0.361	0.352
$T = 65$	0.443	0.435	0.418	0.402	0.391
$T = 85$	<b>0.455</b>	<b>0.460</b>	<b>0.450</b>	<b>0.443</b>	<b>0.437</b>
$T = 95$	0.430	0.410	0.384	0.368	0.356
Ours	<b>0.610</b>	<b>0.608</b>	<b>0.603</b>	<b>0.591</b>	<b>0.580</b>

Table 11: Accuracy of different attack intensity compared with Defensive Distillation on the GTSRB datasets.  $Model_0^{adv}$  represents that the model is trained with clean image and no distillation.  $T$  is the temperature of Defensive Distillation [22]. The best two results are shown in red and blue, respectively.

	$X_1^{adv}$	$X_2^{adv}$	$X_3^{adv}$	$X_4^{adv}$	$X_5^{adv}$
$Model_0^{adv}$	0.545	0.509	0.471	0.449	0.424
$T = 5$	0.522	0.481	0.430	0.409	0.385
$T = 15$	0.543	0.505	0.467	0.448	0.428
$T = 25$	0.499	0.466	0.418	0.404	0.379
$T = 45$	0.512	0.483	0.437	0.422	0.404
$T = 65$	<b>0.558</b>	<b>0.539</b>	<b>0.503</b>	<b>0.489</b>	<b>0.467</b>
$T = 85$	0.504	0.488	0.449	0.435	0.417
$T = 95$	0.518	0.497	0.456	0.438	0.419
Ours	<b>0.667</b>	<b>0.631</b>	<b>0.608</b>	<b>0.598</b>	<b>0.587</b>

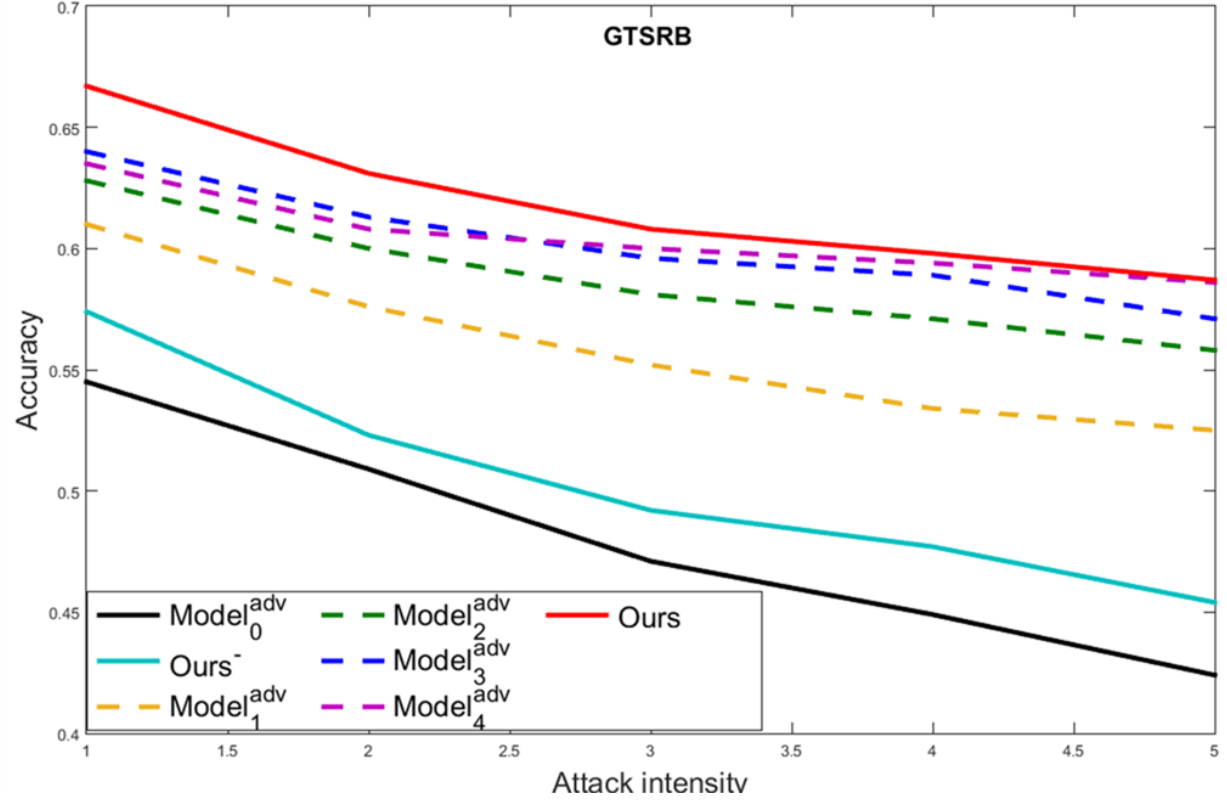


Figure 7: The change curves of accuracy accompanied with attack intensity on the GTSRB dataset.  $Model_0^{adv}$  represents that the model is trained with clean image and no distillation.  $Ours^-$  represents the model is just trained on the CIFAR-10 datasets without trained on the GTSRB datasets in order to convince that the AE-GAN can also gain better performance even if no knowledge of the architecture and the training datasets of the targeted models. **Adversarial training**  $Model_i^{adv}$  represents it had to include all the iterative adversarial examples  $X_0^{adv}, X_1^{adv}, \dots, X_i^{adv}$  to train.  $Ours$  represents the model is trained on GTSRB datasets.

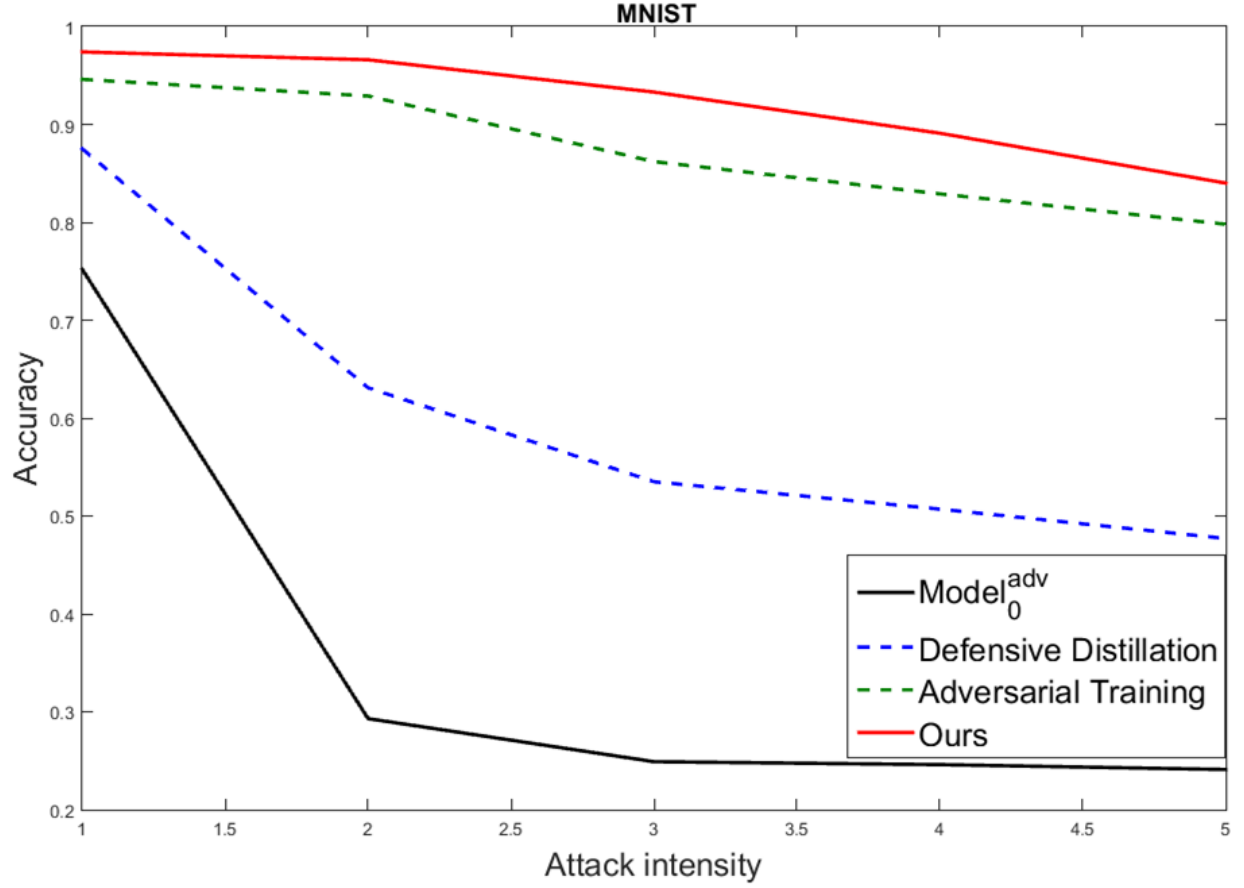


Figure 8: The change curves of accuracy accompanied with attack intensity on the MNIST dataset.  $Model_0^{adv}$  represents that the model is trained with clean image and no distillation. **Defensive Distillation** represents the best result of Defensive Distillation [22]. **Adversarial Training** represents the best result of Adversarial Training [6]. **Ours** represents the adversarial examples should be reconstructed with the AE-GAN before classified by the  $Model_0^{adv}$ .

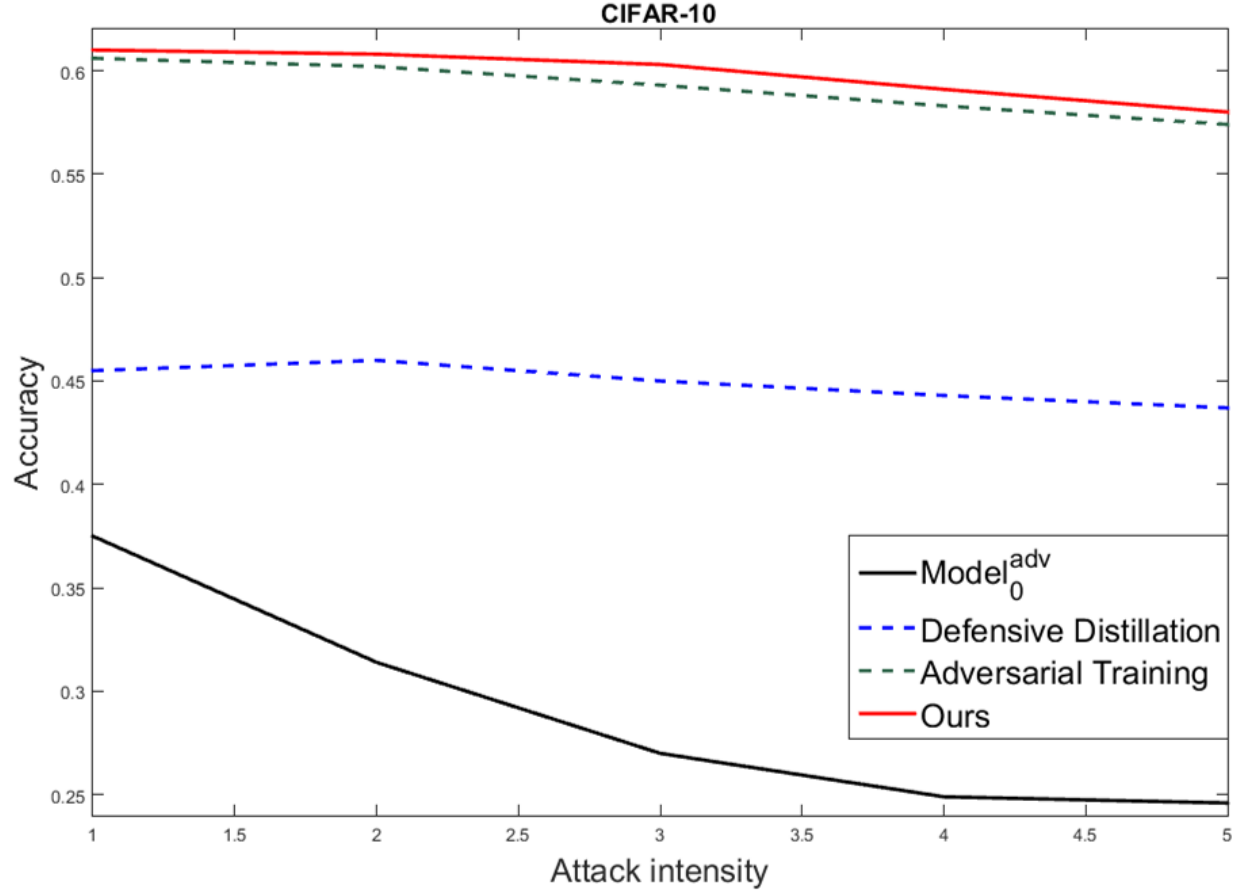


Figure 9: The change curves of accuracy accompanied with attack intensity on the CIFAR-10 dataset.  $Model_0^{adv}$  represents that the model is trained with clean image and no distillation. *Defensive Distillation* represents the best result of Defensive Distillation [22]. *Adversarial Training* represents the best result of Adversarial Training [6]. *Ours* represents the adversarial examples should be reconstructed with the AE-GAN before classified by the  $Model_0^{adv}$ .



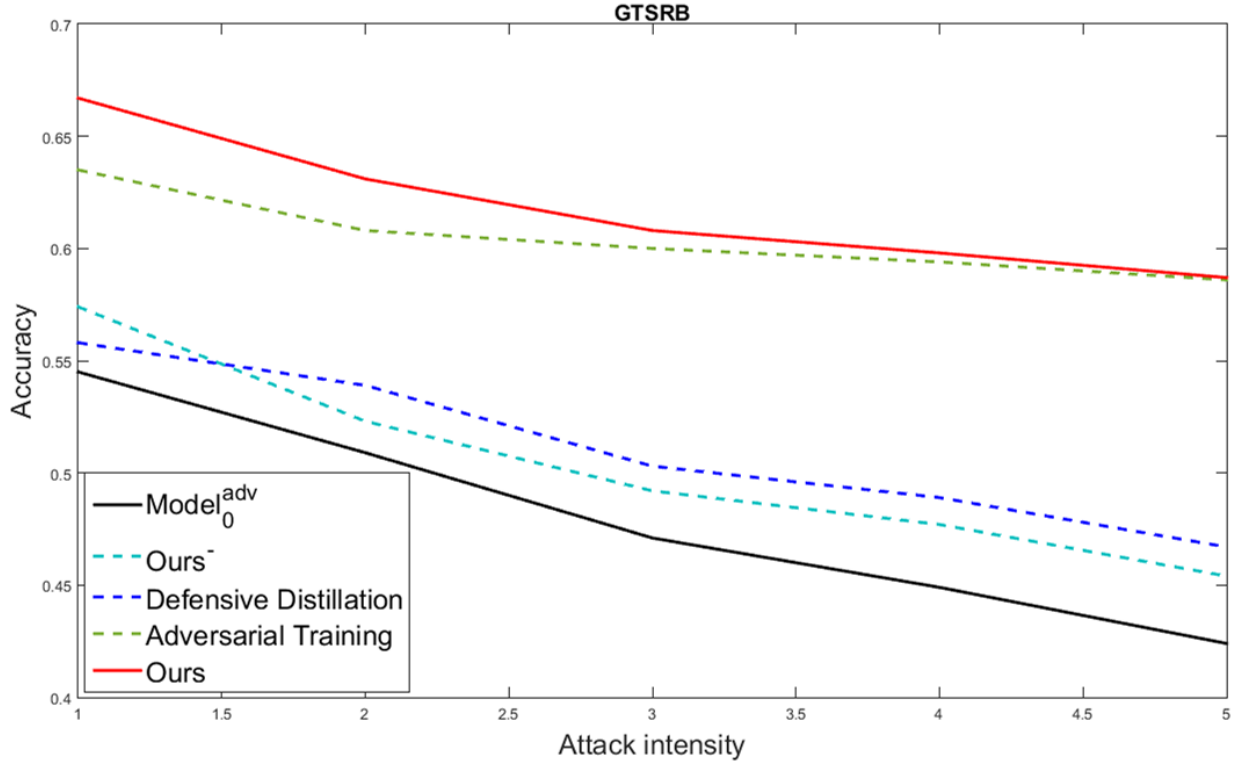


Figure 10: The change curves of accuracy accompanied with attack intensity on the GTSRB dataset.  $Model_0^{adv}$  represents that the model is trained with clean image and no distillation.  $Ours^-$  represents the model is just trained on the CIFAR-10 datasets without trained on the GTSRB datasets in order to convince that the AE-GAN can also gain better performance even if no knowledge of the architecture and the training datasets of the targeted models. **Defensive Distillation** represents the best result of Defensive Distillation [22]. **Adversarial Training** represents the best result of Adversarial Training [6]. **Ours** represents the model is trained on GTSRB datasets.

Table 12: Accuracy of different attack intensity in the MNIST datasets.  $Model_0^{adv}$  represents that the model is trained with clean image and no distillation. *Defensive Distillation* represents the best result of Defensive Distillation [22]. *Adversarial Training* represents the best result of Adversarial Training [6]. *Ours* represents the adversarial examples should be reconstructed with the AE-GAN before classified by the  $Model_0^{adv}$ .

	$X_1^{adv}$	$X_2^{adv}$	$X_3^{adv}$	$X_4^{adv}$	$X_5^{adv}$
$Model_0^{adv}$	0.752	0.293	0.249	0.246	0.241
Defensive Distillation	0.875	0.631	0.535	0.507	0.477
Adversarial Training	0.946	0.929	0.862	0.829	0.798
Ours	<b>0.974</b>	<b>0.966</b>	<b>0.933</b>	<b>0.891</b>	<b>0.840</b>



(a) adversarial samples of the MNIST datasets with  $\epsilon = 15$

Table 13: Accuracy of different attack intensity in the CIFAR-10 datasets.  $Model_0^{adv}$  represents that the model is trained with clean image and no distillation. *Defensive Distillation* represents the best result of Defensive Distillation [22]. *Adversarial Training* represents the best result of Adversarial Training [6]. *Ours* represents the adversarial examples should be reconstructed with the AE-GAN before classified by the  $Model_0^{adv}$ .

	$X_1^{adv}$	$X_2^{adv}$	$X_3^{adv}$	$X_4^{adv}$	$X_5^{adv}$
$Model_0^{adv}$	0.375	0.314	0.270	0.249	0.246
Defensive Distillation	0.455	0.460	0.450	0.443	0.437
Adversarial Training	0.606	0.602	0.593	0.583	0.574
Ours	<b>0.610</b>	<b>0.608</b>	<b>0.603</b>	<b>0.591</b>	<b>0.580</b>



(b) adversarial samples reconstructed by AE-GAN with  $\epsilon = 15$

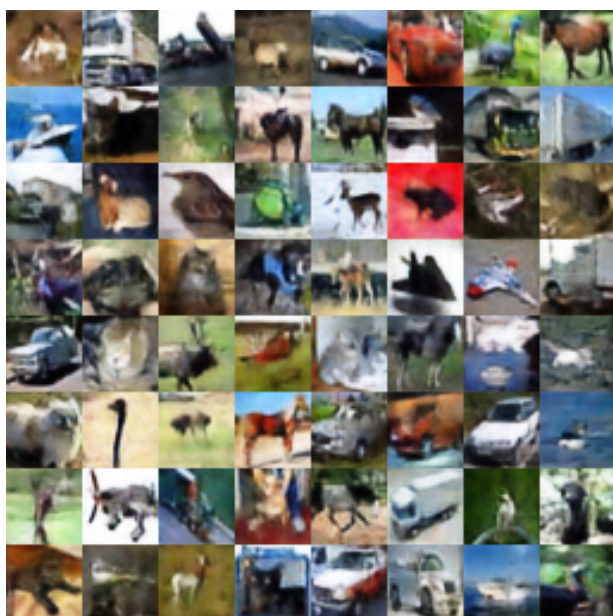
Figure 11: MNIST datasets



(a) adversarial samples of the CIFAR-10 datasets with  $\epsilon = 5$



(a) adversarial samples of the GTSRB datasets with  $\epsilon = 5$



(b) adversarial samples reconstructed by AE-GAN with  $\epsilon = 5$



(b) adversarial samples reconstructed by AE-GAN with  $\epsilon = 5$

Figure 12: CIFAR-10 datasets

Figure 13: GTSRB datasets

Table 14: Accuracy of different attack intensity in the GTSRB datasets.  $Model_0^{adv}$  represents that the model is trained with clean image and no distillation.  $Ours^-$  represents the model is just trained on the CIFAR-10 datasets without trained on the GTSRB datasets in order to convince that the AE-GAN can also gain better performance even if no knowledge of the architecture and the training datasets of the targeted models. **Defensive Distillation** represents the best result of Defensive Distillation [22]. **Adversarial Training** represents the best result of Adversarial Training [6]. **Ours** represents the model is trained on GTSRB datasets.

	$X_1^{adv}$	$X_2^{adv}$	$X_3^{adv}$	$X_4^{adv}$	$X_5^{adv}$
$Model_0^{adv}$	0.545	0.509	0.471	0.449	0.424
$Ours^-$	0.574	0.523	0.492	0.477	0.454
Defensive Distillation	0.558	0.539	0.503	0.489	0.467
Adversarial Training	0.635	0.608	0.600	0.594	0.586
Ours	<b>0.667</b>	<b>0.631</b>	<b>0.608</b>	<b>0.598</b>	<b>0.587</b>

### 4.3 The Generalization of Our Method

The original images, the original images added with random noise and the adversarial examples of different various values of  $\epsilon$  are used as input of our networks in order to validate the generality of our method.

The accuracy of original images, the original images added with random noise are showed in the Table 18 and Table 17. The accuracy of the adversarial examples of different various values of  $\epsilon$  are showed in the Table 15 and Table 16. Figure 14 and the Figure 15 are the experimental renderings.

The Table 17 and Table 18 indicate that our method can ensure that there is no marked decrease in the accuracy of original images and also has a good performance on resist the random noise. In addition, our method can handle various adversarial examples of different intensity according to the Table 15 and Table 16.

## 5 Conclusion

In this paper, we propose a novel idea of defending against adversarial examples via eliminate the trivial perturba-

Table 15: Top-1 accuracy of adversarial images with various noise scale  $\epsilon$  on  $Model_0^{adv}$  and Ours in MNIST datasets. The  $Model_0^{adv}$  represent the original net which just has the clean images to train.

	$Model_0^{adv}$	Ours
$\epsilon = 15$	0.759	0.975
$\epsilon = 20$	0.451	0.963
$\epsilon = 25$	0.241	0.947
$\epsilon = 30$	0.118	0.890
$\epsilon = 35$	0.082	0.851
$\epsilon = 40$	0.063	0.735

Table 16: Top-1 accuracy of adversarial images with various noise scale  $\epsilon$  on  $Model_0^{adv}$  and Ours in CIFAR-10 datasets. The  $Model_0^{adv}$  represent the original net which just has the clean images to train.

	$Model_0^{adv}$	Ours
$\epsilon = 3$	0.392	0.639
$\epsilon = 5$	0.369	0.610
$\epsilon = 7$	0.298	0.566
$\epsilon = 9$	0.226	0.485
$\epsilon = 11$	0.215	0.423

Table 17: The accuracy of the original images and the random noise images in MNIST datasets. The  $Model_0^{adv}$  represent the original net which just has the clean images to train.

	$Model_0^{adv}$	Ours
original images	0.9869	0.9865
random noise images	0.9864	0.9867

Table 18: The accuracy of the original images and the random noise images in CIFAR-10 datasets. The  $Model_0^{adv}$  represent the original net which just has the clean images to train.

	$Model_0^{adv}$	Ours
original images	0.764	0.751
random noise images	0.688	0.732



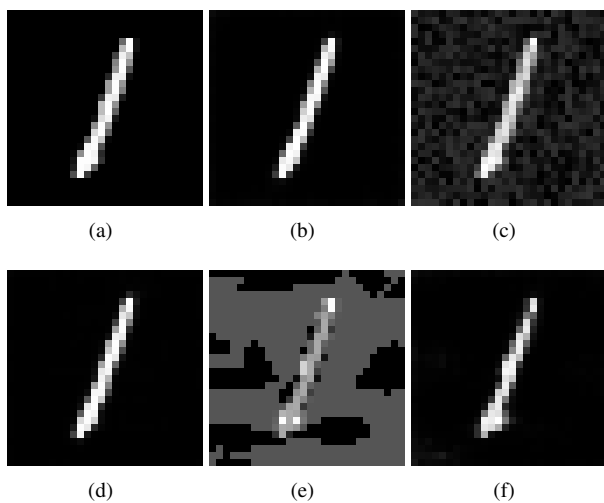


Figure 14: Clean image, random noise image and adversarial samples from MNIST datasets for various values of  $\epsilon$  (a) clean image (b) clean image reconstructed by AE-GAN (c) random noise image (d) random noise image reconstructed by AE-GAN (e) adversarial samples with  $\epsilon = 25$  (f) adversarial samples with  $\epsilon = 25$  reconstructed by AE-GAN

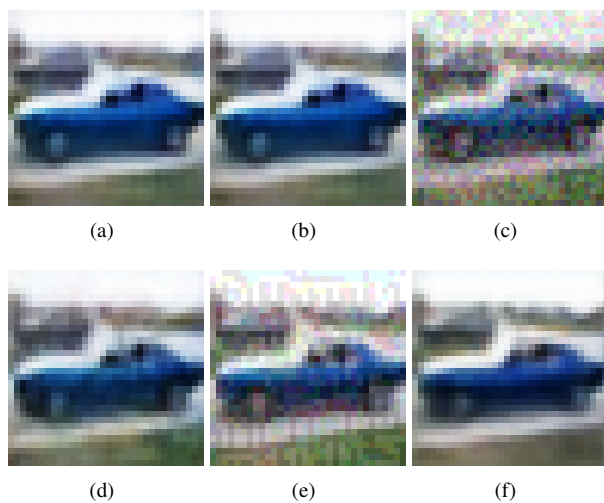


Figure 15: Clean image, random noise image and adversarial samples from CIFAR-10 datasets for various values of  $\epsilon$  (a) clean image (b) clean image reconstructed by AE-GAN (c) random noise image (d) random noise image reconstructed by AE-GAN (e) adversarial samples with  $\epsilon = 5$  (f) adversarial samples with  $\epsilon = 5$  reconstructed by AE-GAN

tions of the input data being highly aligned with the weight vectors of the models. The AE-GAN network is proposed to make the adversarial examples being high consistent with original input image manifold. Future work should deploy new method to eliminate the adversarial perturbation of the adversarial examples.

## References

- [1] B. Biggio, I. Corona, D. Maiorca, B. Nelson, N. Šrđić, P. Laskov, G. Giacinto, and F. Roli. Evasion attacks against machine learning at test time. In *Joint European Conference on Machine Learning and Knowledge Discovery in Databases*, pages 387–402. Springer, 2013. 1
- [2] F. Chollet et al. Keras: Deep learning library for theano and tensorflow. URL: <https://keras.io/k>, 2015. 7, 8
- [3] C. Dong, C. L. Chen, K. He, and X. Tang. Image super-resolution using deep convolutional networks. *IEEE Transactions on Pattern Analysis Machine Intelligence*, 38(2):295, 2016. 6
- [4] C. Farabet, C. Couprie, L. Najman, and Y. LeCun. Learning hierarchical features for scene labeling. *IEEE transactions on pattern analysis and machine intelligence*, 35(8):1915–1929, 2013. 1
- [5] I. Goodfellow, J. Pouget-Abadie, M. Mirza, B. Xu, D. Warde-Farley, S. Ozair, A. Courville, and Y. Bengio. Generative adversarial nets. In *Advances in neural information processing systems*, pages 2672–2680, 2014. 5
- [6] I. J. Goodfellow, J. Shlens, and C. Szegedy. Explaining and harnessing adversarial examples. *arXiv preprint arXiv:1412.6572*, 2014. 1, 2, 4, 13, 14, 15, 16, 18
- [7] S. Gu and L. Rigazio. Towards deep neural network architectures robust to adversarial examples. *arXiv preprint arXiv:1412.5068*, 2014. 1
- [8] G. Hinton, L. Deng, D. Yu, G. E. Dahl, A.-r. Mohamed, N. Jaitly, A. Senior, V. Vanhoucke, P. Nguyen, T. N. Sainath, et al. Deep neural networks for acoustic modeling in speech recognition: The shared views of four research groups. *IEEE Signal Processing Magazine*, 29(6):82–97, 2012. 1
- [9] G. Hinton, O. Vinyals, and J. Dean. Distilling the knowledge in a neural network. *arXiv preprint arXiv:1503.02531*, 2015. 5
- [10] K. Hornik, M. Stinchcombe, and H. White. Multilayer feedforward networks are universal approximators. *Neural networks*, 2(5):359–366, 1989. 1
- [11] S. Houben, J. Stallkamp, J. Salmen, M. Schlipsing, and C. Igel. Detection of traffic signs in real-world images: The German Traffic Sign Detection Benchmark. In *International Joint Conference on Neural Networks*, number 1288, 2013. 7
- [12] D. Kingma and J. Ba. Adam: A method for stochastic optimization. *arXiv preprint arXiv:1412.6980*, 2014. 8
- [13] A. Krizhevsky and G. Hinton. Learning multiple layers of features from tiny images. 2009. 6
- [14] A. Krizhevsky, I. Sutskever, and G. E. Hinton. Imagenet classification with deep convolutional neural networks. In *Advances in neural information processing systems*, pages 1097–1105, 2012. 1
- [15] A. Kurakin, I. Goodfellow, and S. Bengio. Adversarial examples in the physical world. *arXiv preprint arXiv:1607.02533*, 2016. 1, 2, 4
- [16] Y. LeCun, L. Bottou, Y. Bengio, and P. Haffner. Gradient-based learning applied to document recognition. *Proceedings of the IEEE*, 86(11):2278–2324, 1998. 6
- [17] C. Ledig, L. Theis, F. Huszár, J. Caballero, A. Cunningham, A. Acosta, A. Aitken, A. Tejani, J. Totz, Z. Wang, et al. Photo-realistic single image super-resolution using a generative adversarial network. *arXiv preprint arXiv:1609.04802*, 2016. 2
- [18] A. Nguyen, J. Yosinski, and J. Clune. Deep neural networks are easily fooled: High confidence predictions for unrecognizable images. In *Proceedings of the IEEE Conference on Computer Vision and Pattern Recognition*, pages 427–436, 2015. 1
- [19] N. Papernot, I. Goodfellow, R. Sheatsley, R. Feinman, and P. McDaniel. cleverhans v1.0.0: an adversarial machine learning library. *arXiv preprint arXiv:1610.00768*, 2016. 4, 7, 8
- [20] N. Papernot, P. McDaniel, and I. Goodfellow. Transferability in machine learning: from phenomena to black-box attacks using adversarial samples. *arXiv preprint arXiv:1605.07277*, 2016. 1
- [21] N. Papernot, P. McDaniel, I. Goodfellow, S. Jha, Z. B. Celik, and A. Swami. Practical black-box attacks against deep learning systems using adversarial examples. *arXiv preprint arXiv:1602.02697*, 2016. 2, 7
- [22] N. Papernot, P. McDaniel, X. Wu, S. Jha, and A. Swami. Distillation as a defense to adversarial perturbations against deep neural networks. In *Security and Privacy (SP), 2016 IEEE Symposium on*, pages 582–597. IEEE, 2016. 4, 10, 11, 13, 14, 15, 16, 18
- [23] A. Radford, L. Metz, and S. Chintala. Unsupervised representation learning with deep convolutional generative adversarial networks. *arXiv preprint arXiv:1511.06434*, 2015. 5



- [24] C. Szegedy, W. Zaremba, I. Sutskever, J. Bruna, D. Erhan, I. Goodfellow, and R. Fergus. Intriguing properties of neural networks. *arXiv preprint arXiv:1312.6199*, 2013. 1, 4